

# Mechanism of Stabilization of Helical Conformations of Polypeptides by Water Containing Trifluoroethanol

Arthur Cammers-Goodwin, Thomas J. Allen, Sherri L. Oslick, Kim F. McClure, Janette H. Lee, and D. S. Kemp\*

Contribution from the Department of Chemistry, Room 18-582, Massachusetts Institute of Technology, Cambridge, Massachusetts 02139

Received August 22, 1995<sup>®</sup>

**Abstract:** For conjugates Ac-Hel<sub>1</sub>-Ala<sub>n</sub>-OH,  $n = 1-6$ , of the previously characterized reporting, conformational template Ac-Hel<sub>1</sub>, increases in helicity induced by trifluoroethanol (TFE) in water have been related to a simple function of the peptide length  $n$ , yielding the helix propagation constant  $s_{Ala}$ , which increases from 1.0 to 1.5 for  $\chi_{TFE} = 0-20$  mol %. The per-residue helicity increase is similar to the increase in the state stability induced by TFE in monoamide conjugates Ac-Hel<sub>1</sub>-NHR. Addition of TFE to water significantly increases the rate of interconversion of *s-cis/s-trans* amide conformers for Ac-Pro-NHMe, consistent with a significant and selective destabilization of the planar resonance-stabilized amide. In dilute aqueous solution TFE increases helicity by selectively destabilizing amide functions that are solvent exposed, with the consequence that compact conformations such as helices that maximize intramolecular amide–amide hydrogen bonding and minimize amide solvent exposure are selectively favored.

Medium-sized peptides with an intrinsic tendency to assume helical conformations in water often show a dramatic increase in helicity upon addition of relatively low concentrations of certain alcohols, of which the most efficient appears to be trifluoroethanol (TFE). Since its discovery by Goodman and co-workers,<sup>1</sup> this helix-enhancing effect of TFE has found many applications, most recently for NMR-based characterization of short helices derived from natural proteins.<sup>2</sup> Because TFE extends the range of detectable helicity to include polypeptides that are predominantly unstructured in water, titrations with TFE permit comparisons of relative  $\alpha$ -helical propensities between members of peptide series or within regions of the same peptide.<sup>3</sup> Helicity changes resulting from TFE titrations of synthetic peptides have been correlated with amino acid composition, sequence, and helicity-inducing local features.<sup>4,5</sup> Unfortunately, TFE titrations are often difficult to interpret, since

the mechanism by which TFE acts to enhance helicity is widely viewed as uncertain or unknown.<sup>2d,3a,c,d</sup>

A definitive helix enhancement mechanism presumes complete characterization of the effects of TFE on the solvation states of both starting materials and products. Characterization at this level is difficult, since key features of the structure of water itself remain undefined. We address the following practical questions in this report: (1) Which of the two global states is energetically perturbed by TFE? Does TFE selectively raise the energy of the nonhelical random coil state, or lower the energy of the helical state, or both? (2) If the helical state is stabilized, does TFE interact directly with the helix and, if so, with which of its functionalities? (3) If TFE acts by decreasing the stability of the coil state, can the overall stability change be approximated as a sum of effects at each amino acid residue? If it can, does the per-residue effect arise primarily from energy changes involving the amino acid side chains or the amide backbone? (4) Does the TFE effect primarily involve energetic perturbations in electrostatics, hydrophobicity, hydrogen bonding, or some combination of these? Unambiguous answers to these questions should increase our predictive understanding of the effects of TFE on the stability of all folded structures formed by polypeptides.

Twenty five years ago Conio, Patrone and Brighetti examined the helix–coil transition of poly-L-ornithine and poly-L-glutamic acid in water and noted the helix-enhancing effect of aliphatic alcohols. They drew attention to the anomalous thermodynamic properties of water–alcohol solutions and proposed that the likely origin of the helicity enhancement lies in an alcohol-induced decrease in the solvation of solvent-exposed amide groups in the peptide random coil and a consequent selective destabilization of this state.<sup>6</sup> Storrs, Truckses, and Wemmer recently studied the properties in TFE–water mixtures of a helical disulfide conjugate between the peptides apamin and the S-peptide of ribonuclease A and noted that a decrease of

<sup>®</sup> Abstract published in *Advance ACS Abstracts*, March 15, 1996.

(1) (a) Goodman, M.; Listowsky, I.; Masuda, Y.; Boardman, F. *Biopolymers* **1963**, *1*, 33–42. (b) Goodman, M.; Rosen, I. G. *Biopolymers* **1964**, *2*, 537–559. (c) Goodman, M.; Verdini, A. S.; Toniolo, C.; Phillips, W. D.; Bovey, F. A. *Proc. Natl. Acad. Sci. U.S.A.* **1969**, *64*, 444–450.

(2) (a) Dyson, H. J.; Rance, M.; Houghten, R. A.; Wright, P. E.; Lerner, R. A. *J. Mol. Biol.* **1988**, *201*, 201–217. (b) Sönnichsen, F. D.; Van Eyk, J. E.; Hodges, R. S.; Sykes, B. D. *Biochemistry* **1992**, *31*, 8790–8798. (c) Lehrman, S. R.; Tuls, J. L.; Lund, M. *Biochemistry* **1990**, *29*, 5590–5596. (d) Kemmink, J.; Creighton, T. E. *Biochemistry* **1995**, *34*, 12630–12635. (e) Segawa, S.-I.; Fukuno, T.; Fujiwara, K.; Noda, Y. *Biopolymers* **1991**, *31*, 497–509. (f) Jiménez, M. A.; Bruix, M.; Gonzalez, C.; Blanco, F. J.; Nieto, J. L.; Herranz, J.; Rico, M. *Eur. J. Biochem.* **1993**, *211*, 569–581. (g) Shin, H. C.; Merutka, G.; Waltho, J. P.; Tennant, L. L.; Dyson, H. J.; Wright, P. E. *Biochemistry* **1993**, *32*, 6356–6364. (h) Rico, M.; Santoro, J.; Bermejo, F. J.; Herranz, J.; Nieto, J. L.; Gallego, E.; Jiménez, M. A. *Biopolymers* **1986**, *25*, 1031–1053. (i) Gronenborn, A. M.; Bovermann, G.; Clore, G. M. *FEBS Lett.* **1987**, *215*, 88–94. (j) Gronenborn, A. M.; Martin, S. R.; Clore, G. M. *J. Mol. Biol.* **1986**, *191*, 553–561. (k) Carver, J. A.; Collins, J. G. *Eur. J. Biochem.* **1990**, *187*, 645–650. (l) Mammì, S.; Mammì, N. J.; Peggion, E. *Biochemistry* **1988**, *27*, 1374–1379.

(3) (a) Nelson, J. W.; Kallenbach, N. R. *Proteins: Struct., Funct., Genet.* **1986**, *1*, 211–217. (b) Nelson, J. W.; Kallenbach, N. R. *Biochemistry* **1989**, *28*, 5256–5261. (c) Storrs, R. W.; Truckses, D.; Wemmer, D. E. *Biopolymers* **1992**, *32*, 1695–1702. (d) Jasanoff, A.; Fersht, A. R. *Biochemistry* **1994**, *33*, 2129–2135.

(4) (a) Merutka, G.; Stellwagen, E. *Biochemistry* **1989**, *28*, 352–357. (b) Merutka, G.; Stellwagen, E. *Biochemistry* **1990**, *29*, 894–898. (c) Bianco, F. J.; Heranz, J.; Gonzalez, C.; Jimenez, M. A.; Rico, M.; Santoro, J.; Nieto, J. L. *J. Am. Chem. Soc.* **1992**, *114*, 9676–9677.

(5) (a) Bruch, M. D.; Dhingra, M. M.; Gierasch, L. M. *Proteins: Struct., Funct., Genet.* **1991**, *10*, 130–139. (b) Vuilleumier, S.; Mutter, M. *Biopolymers* **1993**, *33*, 389–400.

(6) Conio, G.; Patrone, E.; Brighetti, S. *J. Biol. Chem.* **1970**, *245*, 3335–3340.

temperature and an increase of  $\chi_{\text{TFE}}$  induce similar helicity changes. They adopted the thermodynamic mechanism of Conio et al. and inferred from NMR evidence that direct or indirect stabilizing interactions of TFE with the helical state are unlikely.<sup>3c</sup> In 1994 Jasanoff and Fersht<sup>3d</sup> proposed linear models relating free energy of helix formation to peptide length and  $\chi_{\text{TFE}}$  and drew the opposite conclusion, that a stabilizing interaction between TFE and the helical state is the more plausible mechanism.

In this report we focus attention on TFE solutions in which water is the major component and provide the first direct experimental evidence in support of the thermodynamic explanation of Conio et al. and Wemmer et al. From NMR studies of conjugates of the reporting conformational template Ac-Hel<sub>7</sub><sup>7</sup> we characterize TFE-induced changes in the energetics of formation of single amide–amide intramolecular hydrogen bonds and in the per-residue energetics of helix formation. From NMR and CD studies of the rates of interconversion of s-cis/s-trans amide conformers of acetylproline, we report TFE-induced rate accelerations pertinent to the solvation state of amides.<sup>8</sup>

### Solvation of Conformations of Peptides and Amides in Water–Alcohol Mixtures

Three observations drawn from the vast literature on the solvation of amides, polypeptides, and proteins in water and water–alcohol mixtures are particularly relevant to this analysis: (1) TFE shares its helix-enhancing properties with other alcohols, (2) the magnitude of induced peptide helicity usually depends in a predictable way on the mole fraction of TFE, and (3) TFE–water mixtures exhibit anomalous viscosities, suggestive of a change in water structure.

TFE and other alcohols exert several distinct effects on proteins. At relatively high concentrations in water TFE disrupts hydrophobic interactions, denaturing tertiary and quaternary structure,<sup>9</sup> and in one instance at low concentrations TFE dramatically increases the rate of formation of quaternary structure.<sup>10</sup> Binary mixtures of water with methanol or ethanol also act to denature globular proteins while enhancing helicity in isolated regions of the amino acid sequence,<sup>11</sup> and this property has found recent application in NMR structural studies.<sup>11g,h</sup>

The effects on polypeptides appear to be less complex. Medium-sized peptides with a helical disposition and a low aggregation propensity exhibit enhanced helicity in aqueous TFE solutions, and this property of TFE is shared with other alcohols. The helicities of oligopeptides are also enhanced by aqueous

methanol and ethanol,<sup>6,12</sup> and the efficiency of enhancement is found to increase with the aliphatic chain length of the alcohol.<sup>13a–c</sup> With certain oligopeptides, more complex, concentration-dependent changes are observed. A study of Shibara et al.<sup>13d</sup> of polylysine in solutions of aqueous alcohols showed that low alcohol concentrations induce helicity, but significantly higher alcohol concentrations induce a helix–sheet conformational transition. Among the alcohols TFE is exceptionally efficient in inducing helices in suitable peptide sequences, but it appears to differ from other alcohols only in degree.

For medium-sized polypeptides, relatively low concentrations of TFE induce the most predictable structural changes. Low concentrations are also the most useful for helix induction, since a maximum change in helicity per increment of TFE usually occurs within the range 5–15 mol %, <sup>2a–d,f,i,3a,c,d,5a</sup> and with further increase  $\chi_{\text{TFE}}$  the fractional increase in helicity is usually much less dramatic.

In the earliest helicity studies TFE alone was often used as solvent, advantage being taken of its UV transparency and solvating power,<sup>1</sup> and for many subsequent studies aqueous TFE solutions have been used that contain little water. Since the intrinsic water structure must be strongly perturbed or disrupted at high  $\chi_{\text{TFE}}$ , helical stabilization mechanisms that operate under these conditions are likely to be different and more complex than those operative at low  $\chi_{\text{TFE}}$ . This report deals with the latter cases, in which the medium retains many of the properties of water itself, the helicity changes are largest, and interpretations of experimental results are most likely to be straightforward.

During the past decade Symons and co-workers have systematically studied the structures of alcohol–water mixtures and the capacity of various binary solvent mixtures to hydrogen bond with ketones,<sup>14a,b</sup> phosphine oxides,<sup>14c</sup> and amides.<sup>14d–f</sup> In aqueous mixtures containing up to 20 mol % methanol, Symons et al. find relatively small changes in the solvation environment of amide residues, which is characterized by two donor hydrogen bonds from the protic solvent to the amide oxygen.<sup>14d–f</sup> Although their studies have not included TFE–water mixtures, the similarities in helix enhancement noted above strongly suggest that the solvation properties of amides in methanol–water mixtures will generalize to mixtures containing TFE.

Physical properties of TFE and TFE–water mixtures have been reported by Murto,<sup>15a</sup> Llinas et al.,<sup>15b</sup> and Kallenbach et al.<sup>3a</sup> The bulk dielectric constant  $\epsilon$  of pure TFE is roughly one-third of the value for water, and  $\epsilon$  values for TFE–water mixtures are linear functions of the mole fraction of TFE; thus

(7) (a) Kemp, D. S.; Curran, T. P.; Boyd, J. G.; Allen, T. J. *Org. Chem.* **1991**, *56*, 6683–6697. (b) Kemp, D. S.; Boyd, J. G.; Muendel, C. C. *Nature* **1991**, *352*, 451–454. (c) Kemp, D. S.; Allen, T. J.; Oslick, S. L. *J. Am. Chem. Soc.* **1995**, *117*, 6641–6657. (d) Kemp, D. S.; Allen, T. J.; Oslick, S. L. Submitted for publication. (e) Groebke, K.; Renold, P.; Tsang, K.-Y.; Allen, T. J.; McClure, K. F.; Kemp, D. S. *Proc. Natl. Acad. Sci. U.S.A.*, accepted.

(8) Eberhardt, E. S.; Loh, S. N.; Hinck, A. P.; Raines, R. T. *J. Am. Chem. Soc.* **1992**, *114*, 5437–5439.

(9) Lau, S. Y. M.; Taneja, A. K.; Hodges, R. S. *J. Chromatogr.* **1984**, *317*, 129–140. Miranker, A.; Radford, S. E.; Karplus, M.; Dobson, C. M. *Nature* **1991**, *349*, 633–636. Radford, S. E.; Dobson, C. M.; Evans, P. A. *Nature* **1992**, *358*, 302–307.

(10) Barker, S.; Mayo, K. H. *J. Am. Chem. Soc.* **1991**, *113*, 8201–8203.

(11) (a) Weber, R. E.; Tanford, C. *J. Am. Chem. Soc.* **1959**, *81*, 3255–3260. (b) von Hippel, P. H.; Wong, K.-Y. *J. Biol. Chem.* **1965**, *246*, 3909–3923. (c) Brandts, J. F.; Hunt, L. R. *J. Am. Chem. Soc.* **1967**, *89*, 4826–4838. (d) Inoue, H.; Timasheff, S. N. *J. Am. Chem. Soc.* **1968**, *90*, 1890–1897. (e) Eband, R. M.; Scheraga, H. A. *Biochemistry* **1968**, *7*, 2864. (f) Brown, J. E.; Klee, W. A. *Biochemistry* **1971**, *10*, 470–476. (g) Meadows, R. P.; Nikonowicz, E. P.; Jones, C. R.; Bastian, J. W.; Gorenstein, D. G. *Biochemistry* **1991**, *30*, 1247–1254. (h) Lichtarge, O.; Jardetzky, O.; Li, C. H. *Biochemistry* **1987**, *26*, 5916–5925.

(12) (a) Eband, R. M.; Scheraga, H. A. *Biopolymers* **1968**, *6*, 1551–1571. (b) Yaron, A.; Katchalski, E.; Berger, A.; Fasman, G. D.; Bover, H. A. *Biopolymers* **1971**, *10*, 1107. (c) Conio, G.; Patrone, E. *Biopolymers* **1969**, *8*, 57–68.

(13) (a) Satoh, M.; Fujii, Y.; Kato, F.; Komiyama, J. *Biopolymers* **1991**, *31*, 1–10. (b) Bianchi, E.; Rampone, R.; Tealdi, A.; Ciferri, A. *J. Biol. Chem.* **1970**, *245*, 3341–3345. (c) Bello, J. *Biopolymers* **1993**, *33*, 491–495. (d) Shibara, A.; Yamamoto, M.; Yamashita, T.; Chiouy, J.-S.; Kamaya, H.; Ueda, I. *Biochemistry* **1992**, *31*, 5728–5733. (e) Hermans, J., Jr. *J. Am. Chem. Soc.* **1966**, *88*, 2418–2422. (f) Satoh, M.; Kato, F.; Komiyama, J. *Biopolymers* **1993**, *33*, 985–993. (g) Satoh, M.; Fujii, Y.; Kato, F.; Komiyama, J. *Biopolymers* **1993**, *33*, 1–10.

(14) (a) Symons, M. C. R.; Eaton, G.; Shippey, T. A.; Harvey, J. M. *Chem. Phys. Lett.* **1980**, *69*, 344–347. (b) Symons, M. C. R.; Eaton, G. *J. Chem. Soc., Faraday Trans. 1* **1985**, *81*, 1963–1977. (c) Symons, M. C. R.; Eaton, G. *J. Chem. Soc., Faraday Trans. 1* **1982**, *78*, 3033–3044. (d) Eaton, G.; Symons, M. C. R. *J. Chem. Soc., Faraday Trans. 1* **1988**, *84*, 3459–3473. (e) Eaton, G.; Symons, M. C. R.; Rastogi, P. P. *J. Chem. Soc., Faraday Trans. 1* **1989**, *85*, 3257–3271. (f) Eaton, G.; Symons, M. C. R.; Rastogi, P. P.; O'Duinn, C.; Waghorne, W. E. *J. Chem. Soc., Faraday Trans. 1* **1992**, *88*, 1137–1142.

(15) (a) Murto, J.; Heino, E.-L. *Suom. Kemistil.* **1966**, *B39*, 263–266. (b) Llinas, M.; Klein, M. P. *J. Am. Chem. Soc.* **1975**, *97*, 4731–4737.

at 25 °C and 10 mol % TFE,  $\epsilon$  is 61.0, vs 76.7 for water.<sup>15a</sup> Viscosities of TFE–water mixtures are dramatically nonlinear functions of temperature or of mole fraction. At temperatures below 30 °C a significant viscosity maximum is found in the range of 20–25 mol % TFE; at 25 °C the ratio of  $\eta$  values at ca. 20 and 0 mol % TFE is 2.1, which increases to 2.3 at 15 °C.<sup>15a</sup> Similar but less dramatic viscosity changes are observed for mixtures of water with simple aliphatic alcohols,<sup>15a,16</sup> and these maxima appear to reflect an alcohol-induced restructuring of the hydrogen-bonding interactions of water. In pure TFE a variety of rate and equilibrium effects have been reported;<sup>17</sup> an increase in C-alkylation product is observed for the reaction of allylic halides with sodium phenoxide,<sup>17c</sup> and the slowest rate of interconversion of *s*-cis/*s*-trans amide conformers is seen.<sup>8</sup> More pertinent to the present study, aqueous TFE in the  $\chi_{\text{TFE}}$  0.2 range causes a large decrease in the rate of hydrolysis of picryl fluoride.<sup>17d</sup>

Relative to water, TFE is a much stronger acid ( $\text{p}K_{\text{a}}$  12.4) and a much weaker base.<sup>15</sup> In binary aqueous mixtures of low  $\chi_{\text{TFE}}$ , TFE is likely to interact more strongly with water itself than with other solutes,<sup>17</sup> and at low  $\chi_{\text{TFE}}$  the acidic and basic properties of TFE thus may influence amide solvation only indirectly, by changing the structure of water within the solvation shell, or by increasing either the concentrations or the hydrogen-bonding affinities of Symons defects,<sup>18</sup> which are water molecules with unshared hydrogen-bonding sites.

#### For an N-Templated Ala<sub>n</sub> Homopolymer, $n = 1-6$ , the Helix-Stabilizing Effect of TFE Is a Linear Function of Peptide Length

In solution, a polypeptide helix at equilibrium with a coil state can be modeled by the combined product of an unfavorable initiation parameter  $\sigma$  with a series of marginally favorable propagation parameters  $s$ .<sup>19</sup> We have previously characterized the structure and energetics of short alanine peptides linked to the reporting conformational template Ac-Hel<sub>1</sub> (Figure 1), which assumes the role of helix initiator and permits measurement of changes attributable solely to helix propagation. Of the three conformational states of Ac-Hel<sub>1</sub>, only the *te* state initiates structure in the linked peptide; the peptides linked to *cs* and *ts* template states are experimentally indistinguishable from random coils in water and in water–TFE mixtures.<sup>7c</sup> From NMR and CD evidence the structure of the peptide linked to the template *te* state in these solutions is  $\alpha$ -helical,<sup>7b,d</sup> and the stability of the  $\alpha$ -helix is proportional to the NMR-monitored template  $t/c$  value, which is the concentration ratio of slowly equilibrating template *s*-trans and *s*-cis conformers.<sup>7</sup> This stability relationship is expressed in eq 1, where  $s$  is the average helix propagation constant, and the constants  $A$  and  $B$  are defined as in Figure 1.<sup>7</sup> The geometric series in  $s$  within the parentheses results from the condition that helix nucleation must occur only at the peptide junction. For conjugates Ac-Hel<sub>1</sub>-X<sub>n</sub>-OH,  $n = 1-n$ , we have previously shown that the average helix propagation constant  $s$  can be obtained by an iterative least squares analysis of the length dependence of  $t/c$ , in which  $A$  and  $B$  are

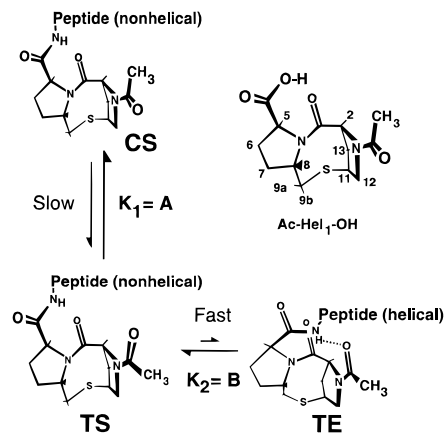


**Figure 1.** The three distinguishable conformational states of an N-terminal conjugate of Ac-Hel<sub>1</sub> with a polypeptide.<sup>7c</sup> Rates are referenced to the NMR time scale.  $A$  and  $B$  are defined as used in eq 1, where  $t/c$  is the concentration ratio of slowly equilibrating *s*-trans and *s*-cis acetamido conformers, measured by integration of *t* and *c* state resonances for the <sup>1</sup>H NMR spectrum in D<sub>2</sub>O.<sup>7c</sup>

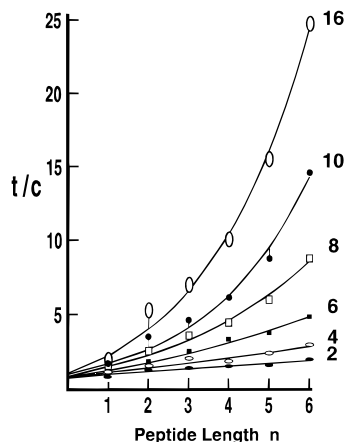


**Figure 2.** Experimental dependence of  $t/c$  on length  $n$  and on mol % TFE for peptide conjugates Ac-Hel<sub>1</sub>-Ala<sub>n</sub>-OH and D<sub>2</sub>O–CF<sub>3</sub>CD<sub>2</sub>OD mixtures at 25 °C. The value of  $t/c$  is related to helicity through eq 1. Points for  $n = 4, 5$ , and  $6$  correspond to measurements at 2, 4, 6, 8, 10, and 16 mol % TFE, as indicated on the right of the graph. Data points for  $n = 1-3$  at low  $\chi_{\text{TFE}}$  are interpolated from measured  $[t]/[c]$  values at 0, 3, 6, 10, and 16 mol % TFE. The curve for 0 mol % TFE (data and curve not shown) is similar to that shown for 2 mol % TFE. Curves are calculated from an iterative least squares data analysis that assigns an  $s_{\text{Ala}}$  for each TFE concentration; data points have an estimated precision of  $\pm 5\%$  of their value.

treated as assignable constants.<sup>7a,b,d,e</sup> Measurements of the effect of TFE concentration on  $t/c$  values thus permit calculation of the magnitude of the TFE-induced change in the helix propagation constant  $s_{\text{Ala}}$ . Since aggregation and diminished solubility prevent study of alanine oligomers with  $n > 6$ , data are reported here for the TFE effect on the  $t/c$  ratio of templated alanine peptides that contain six or fewer amino acid residues. These have previously been shown to be unaggregated in aqueous solutions.<sup>7d</sup>

$$[t]/[c] = A + B(1 + s + s^2 + \dots + s^{n-1}) \equiv A + B(1 + s(1 + s(1 + s(1 + \dots)))) \equiv A + B(s^n - 1)/(s - 1) \quad (1)$$

Figure 2 shows  $t/c$  values measured at 25 °C for Ac-Hel<sub>1</sub>-Ala<sub>n</sub>-OH,  $n = 1-6$ , in D<sub>2</sub>O–TFE binary mixtures, plotted as functions of peptide length for each of a series of mole fractions of TFE. The solid lines of Figure 2 correspond to  $t/c$  values calculated from eq 1 using the  $A$ ,  $B$ , and  $s_{\text{Ala}}$  values obtained

(16) Timmermans, J., Ed. *Physico-Chemical Constants of Binary Systems in Concentrated Solutions*; Interscience: New York, 1960; Vol. 4, p 190.

(17) (a) Leffler, J. E.; Graham, W. H. *J. Phys. Chem.* **1959**, *63*, 687–693. (b) Graybill, B. M.; Leffler, J. E. *J. Phys. Chem.* **1959**, *63*, 1461–1463. (c) Kornblum, N.; Berrigan, P. J.; Le Noble, W. J. *J. Am. Chem. Soc.* **1960**, *82*, 1257–1258. (d) Murto, J. *Acta Chem. Scand.* **1966**, *20*, 303–309.

(18) (a) Symons, M. C. R. *Acc. Chem. Res.* **1981**, *14*, 179–187. (b) Symons, M. C. R. In *Water and Aqueous Solutions*; Neilson, G. W., Enderley, J. E., Eds.; Adam Hilger: Bristol and Boston, 1986; pp 41–55.

(19) Poland, D.; Scheraga, H. S. *Theory of the Helix-Coil Transitions in Biopolymers*; Academic Press: New York, 1970.

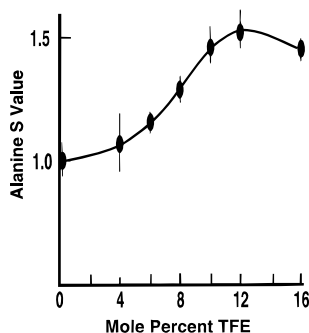


**Figure 3.** Values for  $s_{\text{Ala}}$  in  $\text{D}_2\text{O}$ –TFE mixtures at 25 °C obtained from the  $t/c$  data of Figure 2 by an iterative least squares analysis. Limits of the error bars correspond to  $s_{\text{Ala}}$  values that result in a 15% increase in the sum of squares of the residuals (see Experimental Section).

by iterative least squares analysis. The experimental  $t/c$  values and the derived  $s_{\text{Ala}}$  values of Figure 3 both quantify the large effect of TFE on the helicity of these alanine conjugates. Although the TFE-induced changes in  $s_{\text{Ala}}$  itself may appear small, they translate into large increases in  $t/c$  for  $n = 5$  or 6, owing to the weight of the  $(s_{\text{Ala}})^n$  term within eq 1. The value for  $s_{\text{Ala}}$  in pure water at 25 °C is substantially lower than that reported by Baldwin et al.,<sup>20</sup> but it is in accord with that of Scheraga et al.<sup>21</sup> Elsewhere we have shown that templated alanine-rich heteroconjugates containing 7–15 residues display equivalent  $s_{\text{Ala}}$  values in pure water.<sup>7e</sup>

For  $t/c > 20$  the experimental errors in  $t/c$  increase significantly<sup>7c</sup> and limit the accuracy with which  $s_{\text{Ala}}$  can be defined at high  $\chi_{\text{TFE}}$ . The error bars of Figure 3 imply that the  $s_{\text{Ala}}$  values calculated at high  $\chi_{\text{TFE}}$  are essentially indistinguishable, and the apparent maximum in the graph may therefore be an artifact. However, the data demonstrate unambiguously that  $s_{\text{Ala}}$  is most sensitive to  $\Delta\chi_{\text{TFE}}$  in the mole fraction range of 0.04–0.08 and becomes relatively insensitive above  $\chi_{\text{TFE}} = 0.1$ . This behavior mirrors the previously noted sensitivities of helically disposed untemplated peptides to  $\chi_{\text{TFE}}$ .

The significance of the TFE dependence of the  $t/c$  data is more rigorously demonstrated in Figure 4, in which experimental  $t/c$  values for each alanine conjugate of length  $n$  are plotted as a function of  $\chi_{\text{TFE}}$ . TFE-induced helical cooperativity is seen for  $\text{Ala}_5$  and  $\text{Ala}_6$ , similar to that reported by Kallenbach and Nelson for the S-peptide of ribonuclease A.<sup>3b</sup> The  $t/c$  values that define the curves of Figure 4 were obtained from a model based on eq 1 that uses the  $s_{\text{Ala}}$  values of Figure 3, with  $A$  fixed at 0.79<sup>7c</sup> and  $B$  fixed at an average value for all derivatives studied at a particular TFE concentration (see Experimental Section). This model thus assumes that, at a particular TFE concentration, helix formation is governed by only two parameters, the  $s_{\text{Ala}}$  value, which applies to all amino acid residues except the first, and a template constant  $B$ , which is proportional to the  $s$  value at the template–peptide junction. As seen in Figure 1,  $B$  defines the tendency of the template to assume the *te* state by forming the first hydrogen bond at the junction.

With the exception of data for  $\text{Ac-Hel}_1\text{-Ala}_2\text{-OH}$ , which show significant positive deviations that may be attributable to the conformational readjustments that occur upon addition of the third residue of the first helical loop,<sup>7a,c</sup> all data points of Figure

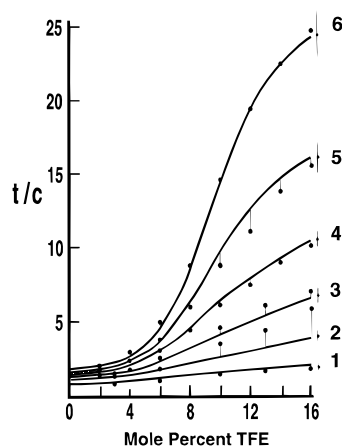


**Figure 4.** Data of Figure 2 for  $t/c$  values of  $\text{Ac-Hel}_1\text{-Ala}_n\text{-OH}$  plotted as a function of mol % TFE and length  $n$ , shown to the right of each curve. For each TFE concentration, points that define the curves are calculated from eq 1 using  $A = 0.79$ ,  $s_{\text{Ala}}$  as shown in Figure 2, and a value of  $B$  that is averaged over  $B$  calculated from eq 1 at fixed [TFE] and  $n = 3, 4, 5, 6$  (see Experimental Section). The error bars shown to the right of each curve are calculated by assuming that the standard deviation in  $B$  is the largest error. From eq 1, a given error  $\Delta B$  in  $B$  is transformed into an error of  $\Delta B(s^n - 1)/(s - 1)$  in  $(t/c)_{\text{calcd}}$ . The deviations seen for  $n = 5$  are in part an artifact of the averaging process, which places the largest weight on the data points for  $n = 6$  (see Experimental Section).

4 lie within the margins of error associated with the model, although small systematic deviations can be noted. Two significant conclusions can be drawn. First, in accord with observations for natural peptides by Jasanoff and Fersht,<sup>3d</sup> for fixed  $\chi_{\text{TFE}}$ , the length-dependent helicity found with this templated peptide series can be modeled to a good approximation by a constant  $s_{\text{Ala}}$  value, the per-residue helical stability increment. The series  $\text{Ac-Hel}_1\text{-Ala}_n\text{-OH}$  stops at  $n = 6$ , but we have seen comparable per-residue helical stabilizations for  $\text{Ac-Hel}_1$  conjugates with alanine-rich heteropeptides containing up to nine backbone NH groups, although the  $t/c$  changes become very large, and the resulting intrinsic errors in  $t/c$  confine the useful measurement range to  $0.0 < \chi_{\text{TFE}} < 0.06$ .<sup>22</sup>

Second, the same stability increment also applies to very short peptide sequences. The responsiveness to TFE shown by  $\text{Ac-Hel}_1\text{-Ala}_3\text{-OH}$  is within error the same as that found for the longer sequences. The tripeptide conjugate bears only the loop at the helix C-terminus, the carbonyl oxygens of which are exposed to solvent. Nevertheless, this derivative exhibits the same per-residue TFE-induced stabilization as larger analogs that retain this C-terminal loop and extend the length of the helix barrel. Relative to residues at the C-terminus, those within the helix barrel must be substantially solvent shielded, and any postulated binding of TFE to discrete elements of helical structure would be expected to show different energetic effects in these two regions. We find no evidence for this difference.

#### For Conjugates $\text{Ac-Hel}_1\text{-NH-R}$ Capable of Forming Only a Single Intramolecular Amide–Amide Hydrogen Bond, TFE in Water Strongly and Selectively Stabilizes the *te* State

The simplest amide derivatives that can be studied as  $\text{Ac-Hel}_1$  conjugates are primary or secondary amides that can form only one intramolecular *te* state hydrogen bond. Figure 5a shows results of TFE titrations of  $\text{Ac-Hel}_1\text{-Ala-OH}$  and similar conjugates  $\text{Ac-Hel}_1\text{-NH-R}$ . The  $t/c$  values in pure  $\text{D}_2\text{O}$  vary substantially for this set of derivatives, with  $\text{Ac-Hel}_1\text{-Ala-OH}$

(20) (a) Chakrabarty, A.; Kortemme, T.; Baldwin, R. L. *Protein Sci.* **1994**, *3*, 843–852. (b) Chakrabarty, A.; Kortemme, T.; Padmanabhan, S.; Baldwin, R. L. *Biochemistry* **1993**, *32*, 5560. Scholtz, J. M.; Qian, H.; York, E. J.; Stewart, J. M.; Baldwin, R. L. *Biopolymers* **1991**, *31*, 1463–1470.

(21) Wojcik, J.; Altmann, K.-H.; Scheraga, H. A. *Biopolymers* **1990**, *30*, 121–134.

(22) Groebke, K.; Kemp, D. S. Unpublished observations.

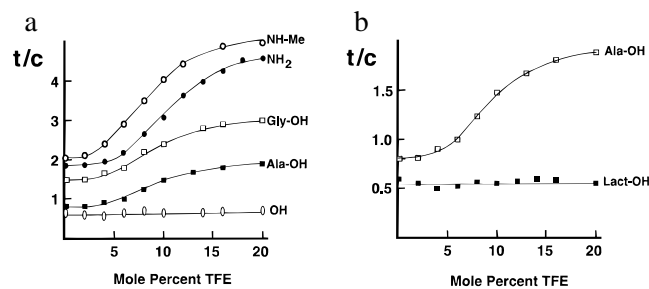


**Figure 5.** Effect of TFE on  $[t]/[c]$  for derivatives Ac-Hel<sub>1</sub>-X in D<sub>2</sub>O at 25 °C. (a) Monoamide series: X = NHCH<sub>3</sub>, NH<sub>2</sub>, NHCH<sub>2</sub>CO<sub>2</sub>H, NHCH(CH<sub>3</sub>)CO<sub>2</sub>H, and OH. (b) Alanine and lactate: X = NHCH(CH<sub>3</sub>)CO<sub>2</sub>H and OCH(CH<sub>3</sub>)CO<sub>2</sub>H.

showing an anomalously small value. However, the increase in  $t/c$  induced by TFE is similar for all members of the series. As with the polyalanine conjugates,  $t/c$  ratios of these monoamides show maximum sensitivity to  $\chi_{\text{TFE}}$  in the range of 0.05–0.1, and the changes in  $t/c$  ratio are accompanied by chemical shift changes in the 2.2–3.3 ppm region that signal the expected increased abundance of the  $t_e$  state relative to the  $t_s$  state (Figure 1). Previously we have attributed this preference to formation of a shorter hydrogen bond in the  $t_e$  state.<sup>7c</sup>

These TFE-induced changes in  $t/c$  imply a large change in state composition;<sup>7c</sup> thus Ac-Hel<sub>1</sub>-NH<sub>2</sub> shifts from 37%  $t_e$  in D<sub>2</sub>O to 66%  $t_e$  in 16 mol % TFE–D<sub>2</sub>O. It is noteworthy that there is no correlation between the magnitude of the TFE effect and the hydrophobic character of the secondary amide N-substituent. One of the largest  $t/c$  changes is seen with the primary amide Ac-Hel<sub>1</sub>-NH<sub>2</sub>, which is the simplest and least hydrophobic member of the series. The state-enhancing effect of TFE clearly is not unique to polypeptides bearing multiple amide residues; a large  $t_e$  state stabilization is also demonstrable with Ac-Hel<sub>1</sub>-NH<sub>2</sub> derivatives that contain only one secondary or primary amide.

Spectra of these derivatives in solution meet the conventional tests for strong solvent shielding of the amide NH function and intramolecular amide–amide hydrogen bond formation. The concentration-independent amide NH stretching frequency seen for Ac-Hel<sub>1</sub>-NHMe in CDCl<sub>3</sub> appears as a broad band centered at 3359 cm<sup>-1</sup>, attributable to the hydrogen-bonded state.<sup>23</sup> In 9/1 H<sub>2</sub>O–D<sub>2</sub>O the temperature dependences of the chemical shifts of  $c$  and  $t$  states of Ac-Hel<sub>1</sub>-NHMe are respectively  $-8.5 \times 10^{-3}$  ppm/K and  $-4.0 \times 10^{-3}$  ppm/K; the latter falls in the range expected for hydrogen-bonded or solvent-shielded amide NH,<sup>24</sup> despite the presence within the  $t$  state average of 38.5%  $t_s$  conformer in which the NH function may be significantly solvent exposed. If one assumes that the experimental temperature dependence observed for the  $c_s$  state also applies to the  $t_s$  state, then the  $t_e$  state dependence is calculated as  $-1.2 \times 10^{-3}$  ppm/K, corresponding to an exceptionally solvent shielded amide NH.

In the temperature range of the study (5–55 °C) the chemical shifts of the  $c$  state and  $t$  state NHs in water lie respectively in the discrete ranges of  $\delta$  7.7–8.1 and  $\delta$  7.3–7.5 ppm. Similar discrete ranges are seen for the nonhelical  $c$  and helical  $t$  state NH resonances of Ac-Hel<sub>1</sub>-Ala<sub>6</sub>-OH.<sup>7b,d</sup> Changes in NH chemical shift upon TFE titration (0–15 mol %) at 25 °C also reflect significantly greater solvent shielding for the  $t$  state: the  $c$  state NH resonance shifts from  $\delta$  7.99 to 7.60 ppm ( $\Delta$ 0.39),

while that of the  $t$  state shifts only from  $\delta$  7.44 to 7.36 ppm ( $\Delta$ 0.08). The  $t$  state resonances show an excellent correlation with the mole fraction<sup>7c</sup> of the  $t_e$  state within the  $t$  state manifold (CC  $-0.99$ ), suggesting that the chemical shifts of both the  $t_s$  and  $t_e$  states may be TFE-invariant. The calculated  $\delta_{t_e}$  in water is 7.30 ppm, which may be compared with a chemical shift value for the  $t$  state in CDCl<sub>3</sub> of 7.24 ppm, implying almost no sensitivity to solvent change. By contrast, the  $c$  state NH resonance is strongly sensitive to solvent. Finally, a NOESY experiment in CDCl<sub>3</sub> shows a  $t$  state cross peak between the NH and the 8-C–H resonances, implying proximity of these protons consistent with the  $t_e$  state structure shown in Figure 1; the  $c$  state resonances lack the corresponding cross peak. Analogous observations have been made for the Ala-1 NH resonances of Ac-Hel<sub>1</sub>-Ala<sub>6</sub>-OH in H<sub>2</sub>O.<sup>7d</sup>

TFE titrations of simple Ac-Hel<sub>1</sub> derivatives that cannot form intramolecular hydrogen bonds provide a further revealing test of the structural requirements for the TFE-induced states changes (Figure 5a,b). The lactate conjugate Ac-Hel<sub>1</sub>-O-CH(CH<sub>3</sub>)-CO<sub>2</sub>H and the acid Ac-Hel<sub>1</sub>-OH show no detectable TFE dependence of  $t/c$ , implying that for these derivatives TFE does not shift the conformational equilibrium to favor the  $t_e$  state. Owing to dominance of the  $s$ -trans conformation at the acyl–oxygen bond of the carboxylic acid function, the simple acid conjugate Ac-Hel<sub>1</sub>-OH lacks the capacity for low-energy intramolecular hydrogen bond formation, and the lactate result shows that the strong TFE dependence seen for Ac-Hel<sub>1</sub>-Ala-OH vanishes if the amide NH is replaced by an ester O. An amide NH function or its equivalent that is solvent-exposed in the  $c_s$  and  $t_s$  states and solvent shielded or intramolecularly hydrogen bonded in the  $t_e$  state appears to be the precondition for a TFE-induced state change.

TFE at 15 mol % induces a 1.5-fold change in  $s_{\text{Ala}}$ , which corresponds to a per-residue  $\Delta\Delta G^\circ$  at 25 °C of  $-0.24$  kcal/mol. For the typical monoamide Ac-Hel<sub>1</sub>-NH<sub>2</sub>, a change in  $\chi_{\text{TFE}}$  from 0 to 16 mol % causes a change in  $K_2$  of Figure 1 of 3.3-fold, corresponding to a  $\Delta\Delta G^\circ$  at 25 °C of  $-0.70$  kcal/mol, or nearly three times the energy increment for  $s_{\text{Ala}}$ . A somewhat larger effect occurs for the atypical Ac-Hel<sub>1</sub>-Ala-OH. We have previously noted that formation of the intramolecular hydrogen bond at the template–peptide junction is unusually favored in water, owing in part to torsional bias at the proline  $\psi$  angle as well as to the unusual hydrophobicity in the vicinity of the template C-5 functionality.<sup>7c</sup>

The per-residue helix-enhancing effect of TFE for helices shows no significant length dependence; the helical per-residue effect is somewhat smaller than the stabilization observed for structures that contain only one secondary or primary amide residue at the template junction, and the presence of at least one such amide residue is a precondition for TFE-induced stabilization. TFE therefore acts by favoring amide states that either are solvent shielded or contain intramolecular amide hydrogen bonds. This finding is inconsistent with selective stabilization of helical structures through direct TFE interaction. TFE thus must act by selectively raising the energy of solvent-exposed amide groups, by default, favoring states containing solvent-shielded or intramolecularly hydrogen bonded amides.

#### Effect of TFE on the Solvation Environment of Simple Amides: TFE in Water Accelerates the Rate of Tertiary Amide $s$ -Cis/ $s$ -Trans Bond Equilibration

A direct experimental test for TFE-induced changes in amide solvation would provide the best independent evidence for the thermodynamic mechanism. Applying an analysis similar to that of Raines et al.,<sup>8</sup> we now show that, in water at relatively

(23) Gellman, S. H.; Dado, G. P.; Liang, G. B.; Adams, B. R. *J. Am. Chem. Soc.* **1991**, *113*, 1164–1173.

(24) (a) Llinas, M.; Klein, M. P.; Niellands, J. B. *J. Mol. Biol.* **1970**, *52*, 399–414. (b) Llinas, M.; Klein, M. P. *J. Am. Chem. Soc.* **1975**, *97*, 473–4737. (c) Dyson, H. J.; Rance, M.; Houghten, R. A.; Lerner, R. A.; Wright, P. E. *J. Mol. Biol.* **1988**, *201*, 161–200.

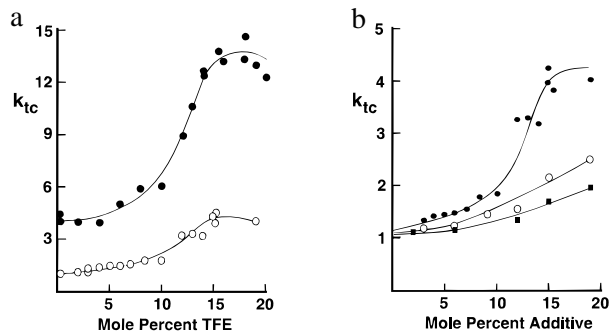
**Table 1.** Absolute and Relative Rate Constants  $k_{tc}$  and Equilibrium Constants  $K_{eq}$  for the Interconversion of *s-trans*- and *s-cis*-Ac-Pro-NHMe in D<sub>2</sub>O Containing 18.9 mol % Additives,  $T = -2$  °C

additive	$(k_{ct} + k_{tc}) \times 10^4$ (s <sup>-1</sup> )	$k_{tc}/k_{ct} =$ $K_{eq}$	$k_{tc} \times 10^5$ (s <sup>-1</sup> )	$k_{tc}/(k_{tc-D_2O})$
D <sub>2</sub> O	2.96 ± 0.07	0.27	6.2	1.0
CD <sub>3</sub> OD	3.30 ± 0.09	0.31	7.7	1.25
DMSO- <i>d</i> <sub>6</sub>	3.8 ± 0.1	0.30	8.7	1.4
C <sub>2</sub> D <sub>5</sub> OD	3.8 ± 0.1	0.36	10.1	1.6
(CD <sub>3</sub> ) <sub>2</sub> CDOD	4.7 ± 0.1	0.37	12.7	2.0
CF <sub>3</sub> CD <sub>2</sub> OD	8.6 ± 0.4	0.32	20.6	3.3

low concentrations, TFE significantly increases the rate at which cis→trans isomerization occurs at the proline tertiary amide bond. The cis→trans isomerizations of the tertiary amide bonds of acyl proline peptides occur slowly, with half-times at 25 °C in the range of 10 s to 60 min,<sup>25</sup> and the rate increases seen with changes from protic to aprotic solvents have been used to model the contribution of desolvation to the catalytic efficiencies of peptidyl prolyl cis→trans isomerases.<sup>26</sup> Grathwohl and Wüthrich have followed rates of change of cis→trans proline amide ratios by <sup>1</sup>H NMR, using either the time course of resonance intensities that follow a rapid change in a ratio-altering experimental variable (e.g., temperature) or saturation transfer between the separate cis and trans NMR resonances.<sup>25b</sup> Raines et al. have used the latter technique.<sup>8</sup>

We have used a simpler method. By X-ray diffraction, Ac-L-Pro-NHMe in the crystalline state exclusively assumes the trans tertiary amide conformation;<sup>27</sup> in water it fails to assume an internally hydrogen bonded  $\gamma$ -turn conformation.<sup>28</sup> Using freshly prepared solutions of this readily soluble material, we have followed the rates of trans → cis isomerization in D<sub>2</sub>O mixtures at -2 and 0.5 °C containing CD<sub>3</sub>OD, C<sub>2</sub>D<sub>5</sub>OD, DMSO-*d*<sub>6</sub>, (CD<sub>3</sub>)<sub>2</sub>CDOD, and TFE-*d*<sub>3</sub> by measuring the time dependence of the ratio of integrated cis and trans <sup>1</sup>H NMR resonances. Similar results were obtained in water-TFE mixtures at 5 °C by following the time dependence of CD ellipticity. These measurements yield values for  $k_{tc} + k_{ct}$ , the sum of the forward (trans to cis) and reverse rate constants for the amide isomerization. Independent NMR measurement of the dependence of the equilibrium constant,  $K_{eq} = k_{tc}/k_{ct}$ , on  $\chi_{TFE}$  allows calculation of the individual rate constants  $k_{tc}$  and  $k_{ct}$  as functions of  $\chi_{TFE}$ . Table 1 lists rate constants  $k_{tc}$  for solutions containing 20 mol % of a series of cosolvents, and Figure 6a compares rate constants for varying  $\chi_{TFE}$ , measured by the NMR and CD techniques at two different temperatures. The dependence of the rate constant on solvent composition for binary mixtures of D<sub>2</sub>O with TFE-*d*<sub>3</sub>, C<sub>2</sub>D<sub>5</sub>OD, and DMSO-*d*<sub>6</sub> is shown in Figure 6b.

The striking finding is that while all these cosolvents increase the rate of isomerization relative to that seen in pure water, the effect is small for CD<sub>3</sub>OD, C<sub>2</sub>D<sub>5</sub>OD, and DMSO-*d*<sub>6</sub> but significantly larger for TFE-*d*<sub>3</sub>. Moreover, for TFE the dependence of slope of  $k_{tc}$  on  $\chi_{TFE}$  is similar to that seen for *t/c* ratios of Ac-Hel<sub>1</sub>-conjugates, consistent with the operation of a common solvation mechanism. The ca. 4-fold rate increase observed with addition of 14–15 mol % TFE may be compared with relative rate increases for the trans → cis isomerization of

**Figure 6.** Experimental rate constants for  $t \rightarrow c$  amide conformational conversion of Ac-L-Pro-NHMe in water mixtures by CD and NMR spectroscopy at 0.5 and 5 °C. Rate constants have an estimated error of 10%, and the curves were drawn to approximate smoothed local averages of the data points. (a) Filled circles:  $k_{tc}$  measured by circular dichroism spectroscopy at 5 °C in TFE–water mixtures. Open circles:  $k_{tc}$  calculated from  $r = [s\text{-cis}]/([s\text{-cis}] + [s\text{-trans}])$ , measured from integrated areas of resonances in the 500 MHz <sup>1</sup>H NMR spectrum at 0.5 °C. The rate constant  $k_{tc}$  was calculated from  $k_{ct} + k_{tc}$ , obtained from the first-order rate analysis of  $r$ , and  $K_{eq}$ , measured after equilibrium was established (see Experimental Section). (b)  $k_{tc}$  measured by <sup>1</sup>H NMR at 0.5 °C: filled circles, data in TFE–water mixtures; open circles, data in C<sub>2</sub>D<sub>5</sub>OD–water mixtures; filled squares, data in DMSO-*d*<sub>6</sub>–water mixtures;  $k_{tc}$  values are in units of 10<sup>-4</sup> s<sup>-1</sup>.

Ac-Gly-Pro-OMe at 50 °C reported by Raines et al., who observe a rate change of roughly 10-fold for a solvent change from water to benzene, dioxane, or toluene. Increasing  $\chi_{TFE}$  in water from 0.0 to 0.15 therefore causes 40% of the rate change expected for a transfer of the amide from water to a nonpolar, aprotic medium.

The progressive increase in rate seen in Table 1 for the series D<sub>2</sub>O, CD<sub>3</sub>OD, C<sub>2</sub>D<sub>5</sub>OD, (CD<sub>3</sub>)<sub>2</sub>CDOD, and TFE-*d*<sub>4</sub> is consistent with the reported tendencies of these alcohols to stabilize helices in small peptides, oligopeptides, and proteins.<sup>11–13</sup> Significant viscosity changes occur in this concentration range, but a mechanism that links these with the observed rate changes is difficult to envisage, and the data themselves argue against a direct correlation of viscosity with rate, since, at 20 mol %, the viscosity<sup>15a,29</sup> of the DMSO mixture is larger than that of TFE, but the former shows a much smaller rate increase for amide bond isomerization. Similarly, within the series of solvents studied, we find no correlation of rate with dielectric constant.

Raines et al.<sup>8</sup> have suggested that the likely origin of the rate effect is a change in hydrogen-bonding state of the amide. For the series of solvents studied, these workers noted a linear correlation between the isomerization rate constant and the amide I C=O stretching frequency. They noted a decrease of ca. 55 cm<sup>-1</sup> in stretching frequency for a series of solvents ranging from toluene and other aprotics to protic solvents that include water; they attributed this decrease to changes in strengths of hydrogen bonds between solvent and the amide function. Although we agree with this interpretation, it appears to be oversimplified. An increase in the strength of polar donor–acceptor interactions other than those attributable to hydrogen bonding is known to cause a significant decrease in amide carbonyl stretching frequency,<sup>14ab,30</sup> and in estimating the portion of the frequency change attributable to the hydrogen-bonding capacity of water, Raines et al. made no correction for a shift attributable to its high dielectric constant. Examining either *N,N*-dimethylacetamide or H-Ala-Gly-OH at 25 °C in binary mixtures of H<sub>2</sub>O and TFE from 0 to 20 mol %, we

(25) (a) Brandts, J. F.; Halvorson, H. R.; Brennan, M. *Biochemistry* **1975**, *14*, 4953–4963. (b) Grathwohl, C.; Wüthrich, K. *Biopolymers* **1981**, *20*, 2623–2633.

(26) (a) Radzicka, A.; Pederson, L.; Wolfenden, R. *Biochemistry* **1988**, *27*, 4538–4541. Radzicka, A.; Acheson, S. A. L.; Wolfenden, R. *Bioorg. Chem.* **1992**, *20*, 382–386. (b) Eberhardt, E. S.; Loh, S. N.; Hinck, A. P.; Raines, R. T. *J. Am. Chem. Soc.* **1992**, *114*, 5437–5439.

(27) Matsuzaki, T.; Iitaka, Y. *Acta Crystallogr.* **1971**, *B27*, 507–516.

(28) Madison, V.; Kopple, K. D. *J. Am. Chem. Soc.* **1980**, *102*, 4855–4863.

(29) Cowie, J. M. G.; Toporowski, P. M. *Can. J. Chem.* **1961**, *39*, 2240–2243.

(30) Bellamy, L. J.; Williams, R. L. *Trans. Faraday Soc.* **1959**, *55*, 14–20.

observe an increase in the amide I infrared C=O stretching frequency of ca. 7  $\text{cm}^{-1}$ , which largely occurs in the range of 6–10 mol % TFE. Unlike the pure solvents examined by Raines et al., the dielectric constants of these solvents are similar. If roughly half of the effect seen by Raines et al. can be attributed to polarity changes, then given that our rate range is 40% of the full range reported by Raines et al., a shift consistent with their data would be  $0.5 \times 0.4 \times 55 = 11 \text{ cm}^{-1}$ , and our observations fall within the range of uncertainty of this estimate. Our results are therefore consistent with the previously reported correlation of exchange rate and stretching frequency.<sup>8</sup>

The hydrogen-bonding environments of amides in protic media have been examined by Eaton and Symons. These workers have introduced simple amides as test molecules into a variety of binary solvent mixtures and have used infrared amide I C=O stretching band multiplicity and variations in the frequency to map the changes in hydrogen-bonding state of the amide oxygen that result from variations in solvent composition. For titration of dimethylacetamide (DMAc) in  $\text{D}_2\text{O}$  with MeOD in the  $\chi_{\text{MeOD}}$  range of 0–0.2, they note only a slight decrease in the amide I C=O absorption peak intensity, little departure from Gaussian shape, and an increase of only 2  $\text{cm}^{-1}$  in frequency.<sup>14c</sup> From other evidence they deduce that the principal amide species in solution under these conditions bears two donor hydrogen bonds from solvent to the amide oxygen. An increase of 16  $\text{cm}^{-1}$  was found to accompany removal of one solvent molecule to form species with a single donor hydrogen bond to the amide oxygen.

Symons, Eaton, et al. have also reported the properties of acetone in binary mixtures of protic and aprotic solvents. As a solute in a series of pure solvents, acetone<sup>14a,b</sup> shows only ca. 40% of the range of C=O stretching frequency seen for DMAc (for the series (water  $\rightarrow$  hexane), acetone,  $\Delta\nu = +24 \text{ cm}^{-1}$  vs  $+64 \text{ cm}^{-1}$  for DMAc; for (DMSO  $\rightarrow$  hexane), acetone,  $\Delta\nu = +13 \text{ cm}^{-1}$  vs  $+33 \text{ cm}^{-1}$  for DMAc). These differences in  $\Delta\nu$  between acetone and DMAc must reflect the greater intrinsic polarity of the resonance-stabilized planar amide, which confers a greater sensitivity to solvent changes.

Formation of the transition state for the interconversion of planar *s-cis* and *s-trans* amide forms involves rotation of the CO–N amide bond to form a nonplanar acetone-like conformer that lacks amide resonance. Increasing the polarity of the solvent must therefore stabilize both the planar *s-cis* and *s-trans* forms to a greater degree than the less polar transition state, increasing the activation energy for the interconversion and retarding the interconversion rate. From their study of pure solvents, Raines et al.<sup>8</sup> have argued that the observed changes in carbonyl stretching frequency and rate constants for *cis*–*trans* isomerization that accompany a change in solvent from protic to aprotic largely reflect the loss of stabilizing hydrogen bonds to the planar amide conformers. This explanation is in accord with the analysis of amide solvation in protic solvents given by Symons et al.<sup>14</sup>

Placed in this context, our observations on binary TFE–water mixtures in the 0–20 mol % range can be interpreted to imply a significant TFE-induced decrease in the strength or abundance of hydrogen bonds between peptide amides and water, resulting in a selective destabilization of solvent-exposed planar amide conformers. Our observations can also be given a more general interpretation, without reference to hydrogen bonding. We have shown that TFE in water causes a significant increase both in the amide C=O stretching frequency and in the rate of *s-cis*/*s-trans* amide interconversion. By these experimental criteria, addition of TFE to water modifies the solvation environment to make it less polar, and TFE therefore must significantly impair

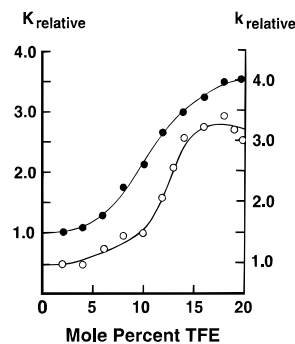


**Figure 7.** Comparison of the effects of TFE on an equilibrium constant ratio and a rate constant ratio. Filled circles and the scale on the left correspond to the TFE-induced shift of state equilibrium at 25 °C to favor the *te* state of Ac-Hel<sub>1</sub>-NH<sub>2</sub>. The data points are calculated as  $(t/c_{\text{TFE-H}_2\text{O}} - 0.79)/(t/c_{\text{H}_2\text{O}} - 0.79)$ , where 0.79 is the value of *A* in Figure 1 and eq 1.<sup>7c</sup> Open circles and the scale on the right represent  $k_{\text{ic(TFE-H}_2\text{O})}/k_{\text{ic(H}_2\text{O})}$  for Ac-L-Pro-NHMe at 5 °C and correspond to the TFE data of Figure 6b. The scales are out of register on the vertical axis to facilitate comparison of curve shapes. The curves were drawn to approximate smoothed local averages of the data points.

the capacity of water to interact with and stabilize the amide function. Accordingly, addition of TFE must disfavor any conformation that bears solvent-exposed amide functions, and by default TFE must favor compact states that contain internally hydrogen bonded or solvent-sequestered amide functions.

## Discussion

Quantitative mechanistic conclusions drawn from different measurements must show consistency. From Figure 7, 15–20 mol % TFE is seen to induce a 3–5-fold increase in the overall equilibrium constant for the formation of a solvent-shielded state as well as a similar change in the rate of *s-cis*/*s-trans* amide isomerization. The comparison shows a striking similarity in the two TFE dependencies. An analogy between the two processes is imperfect, since the transition state for amide *cis*–*trans* rotation is likely to respond differently to TFE than a solvent-shielded amide residue, and the reporter group of acetylprolinamide is a tertiary amide, different in significant respects from the secondary amides of a normal peptide chain. However, these differences cannot obscure the fundamental point that, as measured by the TFE-induced rate differences, the change in amide solvation that results from addition of 15–20 mol % TFE is of sufficient magnitude to explain both the increase in stability of the *te* state of monoamide derivatives of Ac-Hel<sub>1</sub> and the increase in  $s_{\text{Ala}}$  shown in Figure 3. The thermodynamic effect of Conio et al.<sup>6</sup> and Wemmer et al.<sup>3c</sup> has been assessed quantitatively, and its magnitude is consistent with the helicity induced by TFE.

The questions posed in the introduction to this paper can now be addressed. (1) In the  $\chi_{\text{TFE}}$  range of 0.0–0.15 in water, TFE increases helicity by selectively raising the energy of solvent-exposed amide functions of the coil state. (2) We find no evidence for energetically significant stabilization of the helical state by TFE in this  $\chi_{\text{TFE}}$  range. (3) The overall helix stabilization can be approximated as a sum of effects at each amino acid residue, and in the  $\chi_{\text{TFE}}$  range of 0.0–0.15, TFE results in a ca. 50% increase in the value of  $s_{\text{Ala}}$ . (The *s* values for amide functions within the highly hydrophobic environment of Ac-Hel<sub>1</sub> appear to be more susceptible to change by TFE.) From preliminary data, TFE-induced energy changes in the amide backbone appear to dominate side chain effects. For conjugates Ac-Hel<sub>1</sub>-Gly<sub>*n*</sub>-OH, *n* = 1–6, and Ac-Hel<sub>1</sub>-Ala<sub>2</sub>-Xxx-Ala<sub>3</sub>-OH where Xxx = Gly and Leu, TFE at fixed concentration

increases the respective  $s$  values of Ala, Gly, and Leu by a similar multiplicative factor, implying that the free energy of helix propagation per residue is increased by an additive constant that is largely dependent on the TFE concentration and not on the nature of the amino acid side chain.<sup>31</sup> This preliminary result suggests that the helix-inducing effects of TFE may be calculable from a very simple model. (4) Kallenbach and Nelson have previously presented evidence that electrostatic interactions are affected only slightly by TFE.<sup>3</sup> Our results with monoamide derivatives suggest that hydrophobic effects do not assume a primary role in the TFE mechanism, and it is therefore likely that TFE at low concentrations acts primarily to destabilize the interactions between water molecules and backbone or side chain amide functions of polypeptides.

Our experiments have been confined to the binary water–TFE mixtures for which the largest differential changes in helicity are observed. Mechanisms of the helix stabilization effects at much higher TFE concentrations must allow for large changes in dielectric constant, as well as hydrophobic and electrostatic interactions. We do not propose to address these, but one point is noteworthy. Despite considerable scatter in data points, the TFE dependence of  $k_{ic}$  shown in Figure 6 suggests that a  $\chi_{TFE}$  of ca. 0.15 results in a maximum rate of interconversion and that higher TFE concentrations may result in a rate retardation. Consistent with this finding, Raines et al.<sup>8</sup> have shown that, in the absence of water, TFE results in a cis–trans amide isomerization rate that is slower than that seen in water alone. Moreover, as evidenced by shifts in  $\nu_{C=O}$ , the fluorinated alcohols in pure state appear to form stronger hydrogen bonds to amides than water itself.<sup>8,14c</sup> The helix-inducing properties of TFE in largely aqueous mixtures therefore must be attributed to formation within the  $\chi_{TFE}$  range of 0.5–0.15 of a binary solvent complex with special short and medium-range structure that is significantly less efficient at solvating hydrogen bond acceptors than either pure water or pure TFE. The special structure of this complex is reflected in its high viscosity. Data on the effects of alcohols on the rate of hydrolysis of picryl fluoride provide independent evidence pertinent to this conclusion.<sup>17d</sup> TFE in this concentration range was found to retard the rate of hydrolysis significantly, a result that can be interpreted to reflect a TFE-induced decrease in the capacity of the solvent to stabilize incipient fluoride, an ion whose stability is unusually dependent on hydrogen bonding.

Can one draw analogies with the solvation models of Symons et al.<sup>14</sup> to clarify the aqueous solvation changes induced by TFE? These workers have characterized the solvation changes that occur at the carbonyl oxygens of amide solutes in binary mixtures of water, but similar characterization of solvation changes at amide NH functions has proved to be more difficult.<sup>14c</sup> Symons et al. conclude that, in water and its binary mixtures, solvated species with two hydrogen bonds to the amide carbonyl oxygen predominate, and the NH groups of amides are incompletely hydrogen bonded to water. For dimethylacetamide in methanol–water mixtures these workers note that, in the  $\chi_{MeOD}$  range of 0–0.15, methanol causes a small shift away from the doubly hydrogen bonded amide state to the state that bears only one hydrogen bond to the amide oxygen.<sup>14c</sup> A larger shift of this kind would explain the TFE-induced changes we have observed for  $\nu_{C=O}$  and for the rate of amide bond rotation. As Symons et al. note, explanations for these methanol-induced changes are obscure, and a clarification of mechanistic understanding at this level of refinement will require new experimentation.

The most important consequences of our findings are not tied to mechanistic details. Structure induction by TFE that operates by destabilization of solvent-exposed amides is predicted to shift an equilibrium to favor any compact structure that shields amide hydrogen bonding sites from contact with solvent. Moreover, other factors being equal, the degree of stabilization is predicted to be proportional to the number of solvent-exposed amide sites that are shielded. This feature of our stabilization model implies that, for helix formation, TFE should exert most of its influence on helical propagation and should only marginally influence helical initiation (which involves conformational restriction at the  $\phi$  and  $\psi$  angles of three contiguous amino acid residues, together with formation of only one intramolecular hydrogen bond).

This hypothesis of proportionality also suggests a criterion for estimating the relative stabilization induced by TFE in different types of polypeptide secondary structures. Recently,  $\beta$ -hairpins and templated sheet structures derived from peptides have been shown to be stabilized by TFE in water.<sup>32</sup> The  $\beta$ -hairpin is the simplest  $\beta$ -structure; it results from antiparallel sheet formation between the two termini of a single polypeptide that bears a turn at midsequence. This structure can shield a maximum of 50% of its available amide functions through intramolecular hydrogen bonding. By comparison, amide-capped  $\alpha$ -helical peptides of length  $n$  exhibit a shielding of  $100(n-2)/(n+1)$ , which converges to 100% for large  $n$ . An  $\alpha$ -helix of only five residues, capped with amide residues at its termini, thus exhibits a solvent shielding of 50%, equivalent to that of a  $\beta$ -hairpin of any length. By the criterion of maximum solvent shielding of amides, helices are the most compact among regular polypeptide conformations, and they are thus predicted to be most susceptible to TFE stabilization. Undoubtedly for this reason, TFE is frequently observed to induce helicity in fragments of natural proteins that are only partially helical or even nonhelical in the native protein conformation.<sup>2c–e</sup> The  $\alpha$ -helix is not the best of such structures; for a given length, a  $3_{10}$  helix with a solvent shielding of  $100(n-1)/(n+1)$  exhibits the higher fraction of solvent shielding of amide residues. Are TFE-induced helices in fact  $3_{10}$ ? A complete inventory of NOE interactions permits the structure of Ac-Hel<sub>1</sub>-A<sub>6</sub>-OH in TFE–water mixtures to be assigned with confidence as predominantly  $\alpha$ ,<sup>7d</sup> and a similar assignment is likely for the helical C-terminus of a myohemerythrin fragment.<sup>2a</sup> In most cases, the lesser intrinsic stability of the  $3_{10}$  helix when derived from natural amino acid residues probably outweighs the gain from a small increase in solvent shielding in converting  $\alpha$  to  $3_{10}$ .

More generally, for a given polypeptide, a strong sequence or aggregation-derived bias toward a particular solvent-shielded conformation is likely to outweigh the per-residue advantage offered by a helical structure, even though the latter shields a higher percentage of amide sites. This balance between competing structures must explain the tendency of certain sequences to assume  $\beta$ -structure or to aggregate in water in the presence of low concentrations of TFE.

In this study we have only examined amide–amide interactions, and many experimentally resolvable issues remain. Does TFE also shift equilibria to favor hydrogen bonds between amides and other hydrogen bond donors such as alcohols and ammonium ions? Does it favor weak or distorted amide–amide

(31) Allen, T. J.; Kemp, D. S. Unpublished observations.

(32) (a) Balcerski, J. S.; Pysh, E. S.; Bonora, G. M.; Toniolo, C. *J. Am. Chem. Soc.* **1976**, *98*, 3470–3473. (b) Blanco, F. J.; Jiménez, M. A.; Pineda, A.; Rico, M.; Santoro, J.; Nieto, J. L. *Biochemistry* **1994**, *33*, 6004–6014. (c) Blanchard, D. E.; Arico-Muendel, C.; Bieganski, R.; Kemp, D. S. Unpublished observations.

(33) Hamilton, W. C. *Statistics in Physical Science*; The Ronald Press Company: New York, 1964; pp 124–132.

hydrogen bonds that are solvent exposed? A stability paradox also awaits clarification. The maximum  $s$  value for a single alanine residue in TFE–water mixtures is 1.5, which is sufficient to offset the helix-breaking effect of a neighboring residue with an  $s$  value in the range of 0.6–0.7. If TFE enhances the helical propensities of all amino acid residues by a constant multiplicative factor, for most peptides the resulting large value of  $\sigma s^{n-2}$  is calculated to override the low intrinsic helicities of local regions, and the stabilities for long, continuous polypeptide helices are predicted to be very large. Yet for particular polypeptides TFE is recognized to be incapable of extending helical structure beyond specific regions.<sup>3</sup> Strengthening by TFE of certain stop signals is a likely explanation. Finally, understanding of TFE-induced peptide aggregation phenomena will require characterization of changes in the aqueous hydrophobic effect in the presence of TFE.

## Summary

With Ac-Pro-NHMe, in the 0–15 mol % range in water, TFE increases the rate of *s*-cis/*s*-trans equilibration at the tertiary amide bond. At a fixed concentration in water, TFE shifts the conformational equilibrium to favor solvent-shielded amide conformations for a series of derivatives Ac-Hel<sub>1</sub>-NHR. With the series Ac-Hel<sub>1</sub>-Ala<sub>*n*</sub>-OH,  $n = 1-6$ , TFE also induces a constant per-residue stabilization of  $\alpha$ -helices. The magnitudes of these three effects are similar. As suggested by Conio et al.<sup>6</sup> and by Wemmer et al.,<sup>3c</sup> TFE in the 0–15 mol % range in water acts by diminishing stabilization of water-exposed amide functions, shifting equilibria away from highly solvated coil states toward compact states that contain internally hydrogen bonded or solvent-sequestered amides.

## Experimental Section

Reagents were purchased or purified as described previously, and all Ac-Hel<sub>1</sub> derivatives were prepared, purified, characterized, and analyzed by <sup>1</sup>H NMR spectroscopy at 500 MHz as reported previously.<sup>7c</sup> Ac-L-Pro-NHMe was prepared and purified as reported by Madison and Kopple.<sup>28</sup> Although agreement between  $t/c$  values averaged over several spectroscopic regions gives a higher precision,<sup>7c</sup> we estimate the accuracy of the  $t/c$  data at  $\pm 5\%$  of the value of the data point.

**Least Squares Analyses of  $t/c$  Data Blocks from Ac-Hel<sub>1</sub>-Ala<sub>*n*</sub>-OH.** To obtain constants  $A$  and  $B$  from a least squares fit<sup>32</sup> to eq 1, programs of Mathematica 2.0 were employed to solve the matrix equation  $\mathbf{z} = \text{inverse}[(\text{transpose}[\mathbf{x}])(\text{inverse}[\mathbf{m}])\mathbf{x}] \cdot [(\text{transpose}[\mathbf{x}]) - ((\text{inverse}[\mathbf{m}])\mathbf{y})]$ , where  $\mathbf{y}$  is defined as the  $t/c$  data vector for  $n = 1-6$ , including the  $n = 0$  data point of  $t/c = 0.79$ ;  $\mathbf{x} = \{1, 1, 1, (s^2 - 1)/(s - 1), 1, (s^3 - 1)/(s - 1), 1, (s^4 - 1)/(s - 1), 1, (s^5 - 1)/(s - 1), 1, (s^6 - 1)/(s - 1)\}$ ,  $\mathbf{z} = \{A, B\}$ , and  $\mathbf{m}$  is the variance–covariance matrix, which in this study can only be approximated to within a scale factor. Since the  $t/c$  ratios are unlikely to be correlated, within  $\mathbf{m}$  all covariances (off-diagonal terms) were set equal to 0. The variances that appear along the diagonal of  $\mathbf{m}$  were taken as proportional to the  $t/c$  ratio itself. Negligible changes in modeling outcome were noted when the diagonal terms were replaced by  $(t/c)^{0.5}$ .

Values of  $s_{\text{Ala}}$  reported in Figure 3 were obtained by repetition of the above analysis with systematic variation of  $s$  to obtain the minimum value of the sum of squares of errors in the residuals:  $\sum(t/c_{\text{exptl}} -$

$t/c_{\text{calcd}})^2$ , where  $t/c_{\text{calcd}}$  is obtained from eq 1 using the constants  $A$  and  $B$  obtained from  $\mathbf{y}$  of the above analysis. Errors in  $s_{\text{Ala}}$  obtained by this iterative procedure were set at the limiting values of  $s_{\text{Ala}}$  required to increase the above error term by 15%; these are shown in Figure 3.

**Data Analysis for Figure 4.** To calculate averaged  $B$  values used in Figure 4, the optimized  $s_{\text{Ala}}$  at fixed TFE concentration was used to calculate  $(s_{\text{Ala}}^n - 1)/(s_{\text{Ala}} - 1)$  values corresponding to each measured  $t/c$  value for the series Ac-Hel<sub>1</sub>-Ala<sub>*n*</sub>-OH,  $n = 3-6$ . The constant  $A$  was set equal to 0.79 as noted previously,<sup>7c</sup> and the measured  $t/c$  values were combined with the above  $s$  terms to obtain a  $B$  value for each Ala derivative, using eq 1. The average of these  $B$  values was used with  $A = 0.79$  and the experimental  $s_{\text{Ala}}$  to calculate the curves shown in Figure 4. The following  $B$  values (with SD) were obtained: 16 mol % TFE, 1.28 (0.07); 12 mol %, 0.855 (0.10); 10 mol %, 0.73 (0.08); 8 mol %, 0.62 (0.06); 6 mol %, 0.48 (0.03); 4 mol %, 0.30 (0.06).

**<sup>1</sup>H NMR Kinetic Analysis.** Ac-L-Pro-NHMe was crystallized from CHCl<sub>3</sub> and powdered, and ca. 10 mg was taken up in the NMR solvent at 0 °C within the cooled NMR tube and transferred to the probe of the Varian 500 MHz NMR spectrometer. A single pulse spectrum was taken every minute for the first 20 min, then every 2 min thereafter. The variable temperature control of the probe was calibrated using the difference between the chemical shifts of the OH and CH resonances of methanol. The progress of the isomerization was monitored by following the integration ratios of the amide *N*-methyl and Pro  $\alpha$ -CH resonances. The equilibrium ratio  $y = k_{\text{tc}}/k_{\text{ct}}$  of *cis* and *trans* amide conformers was determined from integration ratios of the resonances after 20 h. Digitized data from NMR integration were used to plot time vs  $\ln(X_{\infty}/X_{\infty} - X_t)$ , where  $X_{\infty}$  and  $X_t$  are  $[\text{cis}]/([\text{cis}] + [\text{trans}])$  at infinite time and time  $t$ , respectively. The slope of this plot yields  $(k_{\text{tc}} + k_{\text{ct}}) = x$ ;  $k_{\text{tc}}$  is calculated from the relationship,  $k_{\text{tc}} = xy/(y + 1)$ .

**CD Kinetic Analysis.** With the exception that 2 mg samples of Ac-L-Pro-NHMe were used to prepare a solution at 5 °C that was diluted to 3 mM for spectroscopy in a 1 mm quartz cell, samples were prepared as described above. CD analysis was carried out in a thermostated cell block of an Aviv Model 62DS CD spectrometer, and data were analyzed as described above. Errors in rate constants were roughly 10%.

**Infrared Spectroscopy in TFE–Water Solutions.** A Perkin-Elmer FT infrared spectrometer Model 1600, equipped with a horizontal trough attenuated total reflectance zinc selenide cell (HATR, SpectroTech), was used. TFE, Aldrich spectroscopic grade, 99+%, was used without further purification; Ala-Gly was purchased from Fluka AG and used without further purification. A stock solution of Ala-Gly in water (380  $\mu\text{L}$  of 0.53 M) was diluted with an appropriate amount of TFE and water. A solvent blank and the Ala-Gly solution were scanned using the HATR cell to yield subtracted spectra. The wavenumbers of the carbonyl peaks were determined at 12 different  $\chi_{\text{TFE}}$  in the range of 0–0.3. Identical experiments were carried out, replacing Ala-Gly with dimethylacetamide. Ten to twelve data points were taken, and carbonyl frequencies were reproducible within  $\pm 1.5 \text{ cm}^{-1}$ . A plot of  $\nu_{\text{C=O}}$  vs  $\chi_{\text{TFE}}$  showed a large positive slope in the region of  $\chi_{\text{TFE}}$  from 0.0 to 0.08 and significantly decreased positive slope above 0.09.

**Acknowledgment.** Fellowship support for K.F.M., NIH Grant 5 F32 GM15837-02, and financial support from the NIH, Grants 5 R01 GM 40547 and R37 GM 13453, from the NSF, Grant No. 9121702-CHE, and from Pfizer Research are gratefully acknowledged.

JA952900Z